Available online at www.sciencedirect.com

SciVerse ScienceDirect

Ceramics International 39 (2013) 5725–5732

CERAMICS INTERNATIONAL

www.elsevier.com/locate/ceramint

The effect of titanium bead diameter of porous titanium on the formation of micro-arc oxidized TiO_2-based coatings containing Si and Ca

Rui Zhou[a], Daqing Wei[a,*,1], Su Cheng[b], Yu Zhou[a,*], Dechang Jia[a], Yaming Wang[a], Baoqiang Li[a]

[a]*Institute for Advanced Ceramics, Department of Materials Science and Engineering, Harbin Institute of Technology, Harbin 150001, PR China*
[b]*Department of Mechanical Engineering, School of Architecture and Civil Engineering, Harbin University of Science and Technology, Harbin 150001, PR China*

Received 6 November 2012; received in revised form 26 December 2012; accepted 29 December 2012
Available online 9 January 2013

Abstract

Porous titanium was prepared by vacuum sintering titanium beads with diameters of 100, 200, 400 and 600 μm on titanium plate at temperature 1723 K for 2 h. Then TiO_2-based coatings containing Si, Ca, Na (SCN) elements were fabricated by micro-arc oxidation (MAO) on the porous titanium. The results showed that the surface morphology, SCN concentrations and x-ray diffraction intensity of titania of the MAO coatings were significantly affected by titanium beads diameter. With increasing titanium beads diameter, the porosity of porous titanium raised gradually in a range of 26.5%–35% and the specific surface area of porous titanium decreased gradually in a range of 45%–5% mm^{-1}. The oxidizing ability is positive correlated with bead diameter as porosity but negative correlated with bead diameter as specific surface area. In this paper, the porosity and specific surface area are two key factors to influence the formation and microstructures of MAO coatings.

Keywords: D. TiO_2; Bead diameter; Microarc oxidation; Porous titanium

1. Introduction

Porous titanium has been widely studied for orthopedic and dental implants application because of its good biocompatibility, nice corrosion resistance, low elastic modulus (close to bone) and porous structure which provide good biological fixation to the surrounding tissue [1–3]. However, titanium and its alloys have poor osteoinductive properties because of their bioinert feature [4–6]. Thus, preparing bioactive coatings is an approach to resolve the disadvantages of porous titanium and its alloys. Microarc oxidation (MAO) is a relatively convenient and effective technique to deposit ceramic coatings on the surfaces of Ti, Al, Mg and their alloys [7]. This technique can introduce various desired elements into MAO coatings and produce various functional coatings with a porous structure [7–12]. Using MAO technique to deposit bioactive ceramic coatings on titanium and its alloys has received much attention in recent years [13–18]. However, most MAO coatings were formed on the flat substrates, and the researches on the formation of MAO coatings on the porous titanium have less reported.

A number of approaches to fabricate three-dimensionally porous titanium have been reported, including partial sintering of powders [19] or wires [20], sintering of powders around a temporary space-holding phase [21,22], and selective laser or electron beam melting [23–25]. Among these techniques, selective laser or electron beam melting can control the porosity and pore size of the materials, but the quality of structure is hard to be controlled. It is affected by various

*Corresponding authors. Tel.: +86 451 8640 2040; fax: +86 451 8641 4291.
E-mail address: daqingwei@hit.edu.cn (D. Wei).
[1]Postal address: P.O. Box 3022#, Institute for Advanced Ceramics, Science Park, Harbin Institute of Technology, Yikuang Street, Harbin 150080, PR China.

0272-8842/$ - see front matter © 2013 Elsevier Ltd and Techna Group S.r.l. All rights reserved.
http://dx.doi.org/10.1016/j.ceramint.2012.12.090

factors, such as geometry of the structure, powder characteristics and melting parameters [23]. Compared to the above methods, vacuum sintering of titanium beads to fabricate porous titanium has obvious advantages. It can not only produce porous materials with high porosity and well interconnected structure, but also easily control the porosity and specific surface area of porous titanium by choosing diameter of titanium bead.

In this study, four kinds of porous titanium with different porosity and specific surface area made by titanium beads of different diameters were treated by MAO. The elements of Si, Ca and Na (SCN) were introduced into the MAO coatings. It has been proved that the MAO coatings on titanium plate containing SCN possessed good biocompatibility in our previous works [26–28]. Now we focus on the influence of porous structure on the structure of MAO coatings containing SCN.

2. Experimental procedure

2.1. Specimens preparation

Four kinds of commercial titanium beads with diameters of 100, 200, 400 and 600 μm supplied by Baoji Haibao special metal materials co., Ltd. of China were sintered to fabricate porous titanium. Fig. 1 shows the schematic diagram for the structure of the porous titanium prepared by vacuum sintering titanium beads. The porous Ti layer with thickness of 0.4–0.6 mm were prepared by using titanium beads to be sintered on titanium plates ($30 \times 30 \times 1$ mm^3), where the titanium plates were ground with 400#, 800# and 1000# abrasive papers, washed with acetone and distilled water, and dried at 40 °C. The Ti plates covered by titanium beads with four different particle sizes were filled in a graphite mold. BN lubricant was sprayed on the inner wall of the mold to avoid the reaction between graphite and Ti during sintering. At last, the samples were sintered under vacuum environment (10^{-3} Pa) without applied pressure by holding at temperature 1723 K for 2 h with a heating rate of 10 °C/min.

The Ti plates covered titanium beads (labeled as MAO100, MAO200, MAO400, MAO600 according to the titanium beads diameters of 100, 200, 400 and 600 μm) were used as anodes, and stainless steel plates were used as cathodes in an electrolytic bath. An electrolyte was prepared by the dissolution of reagent-grade chemicals of $Ca(CH_3COO)_2 \cdot H_2O$ (6.3 g/l), Na_2SiO_3 (13.2 g/l), EDTA-2Na (15 g/l) and NaOH (15 g/l) into deionized water. The applied voltage of 500 V was used to prepare MAO coatings on substrates. The frequency, duty cycle and oxidizing time were 600 Hz, 8.0% and 5 min respectively. The temperature of the electrolyte was kept at 40 °C by the cooling system.

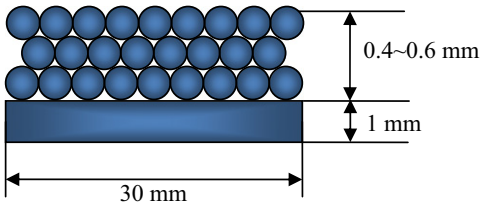

Fig. 1. Schematic diagram for the structure of the porous titanium prepared by vacuum sintering titanium beads on titanium plate.

2.2. Structure characterization

2.2.1. X-ray diffraction (XRD)

The phase composition of MAO samples were analyzed by X-ray diffraction (XRD, D/max-gB, Japan) using a Cu Ka radiation with a continuous scanning mode at a rate of 4°/min, under an accelerating voltage of 40 kV and current of 50 mA.

2.2.2. Scanning electron microscopy (SEM) and energy dispersive X-ray spectrometer (EDS)

Scanning electron microscopy (SEM, Quanta 200, FEI Co., American) was used to observe the surface morphologies. In addition, the elemental concentrations of the surface of samples were detected by an energy dispersive X-ray spectrometer (EDS, EDAX, American) equipped on the SEM system. The SEM micrographs of the surface morphologies of the specimens were subjected to image analysis to measure the micropore numbers and sizes.

2.2.3. The porosity and specific surface area

The sintered porous samples were immersed into the melted olefin, which was filled into the pores of porous titanium. Then the temperature decreased to solidify the melted olefin in the pores of porous titanium. The solidified sample was ground to reach the same size compared to that before immersion. At last the drainage method was used to determine the volumes of sintered porous samples non- and containing olefin. The porosity was calculated by the following equation:

$$\text{Porosity} = (V - V_1)/V \times 100\% \quad (1)$$

where V_1 and V are the volumes of sintered porous samples non- and containing olefin

The shape and size of sample are shown in Fig. 1, and the specific surface area was calculated by the following equation:

$$\text{Specific surface area} = S_s/V_1 \quad (2)$$

where the S_s is the sum surface area of sample.

2.2.4. The current density

The current density during the MAO process was calculated by following equation:

$$\text{Current density} = I/S_s \quad (3)$$

where I is the current intensity during the MAO process.

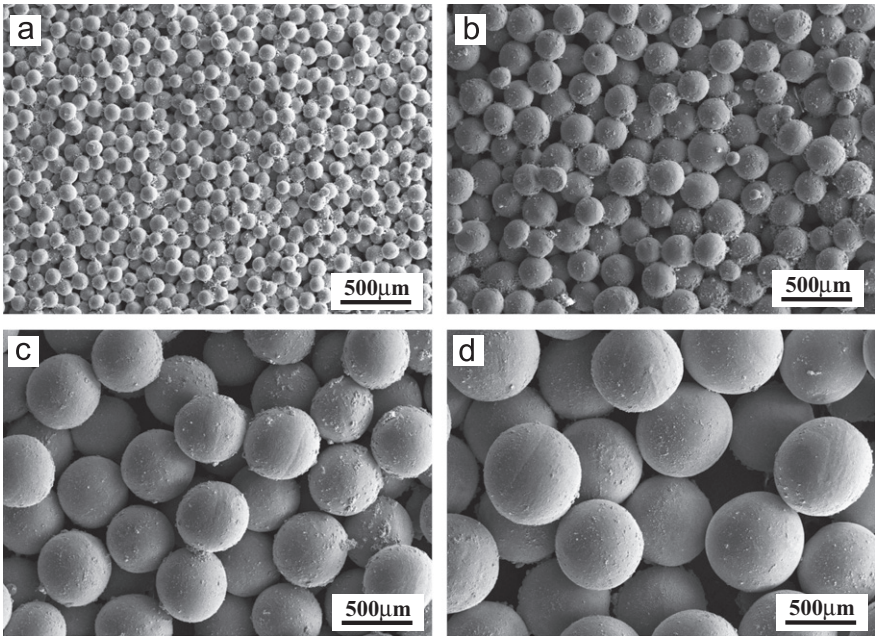

Fig. 2. SEM morphology of the porous titanium prepared by vacuum sintering titanium beads with different diameters: (a) MAO100, (b) MAO200, (c) MAO400 and (d) MAO600.

3. Results

3.1. Surface morphology of porous titanium before MAO treatment

Fig. 2 shows SEM morphology of the porous titanium prepared by vacuum sintering titanium beads with different diameters of 100, 200, 400 and 600 μm. No obvious changes in diameter of titanium beads were observed after sintering. And the size of pores among titanium beads increased obviously as an increase in the diameter of titanium beads.

Fig. 3 shows the porosity and specific surface area of porous titanium prepared by sintering titanium beads with different diameters of 100, 200, 400 and 600 μm. With increasing of the titanium beads diameter from 100 to 600 μm, the porosity of porous titanium increased gradually in a range of 26.5%–35%, while the specific surface area of porous titanium decreased gradually in a range of 45%–5% mm^{-1}.

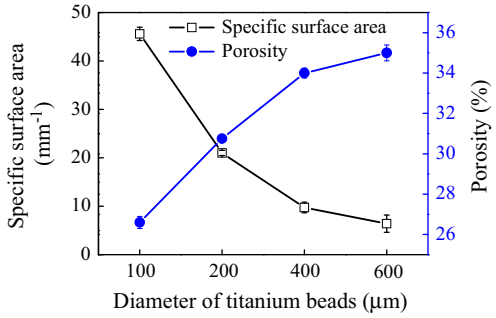

Fig. 3. Porosity and specific surface area of porous titanium prepared by vacuum sintering titanium beads with different diameters of 100, 200, 400 and 600 μm.

3.2. Current density of the MAO process

Fig. 4 shows the changes in the current density during the MAO process for various porous titanium substrates prepared by vacuum sintering titanium beads with diameters of 100, 200, 400 and 600 μm. Totally, the changes of MAO current density can be divided to two stages of boosting voltage and constant voltage. Generally, the current density increased at the stage of boosting voltage. Conversely, it decreased at the stage of constant voltage due to the formation and growth of the MAO coatings. However, it was obvious that the current density in the MAO process for MAO400 sample was the highest compared to the other sample. This result suggestes that the reaction intensity during the MAO process for MAO400 sample is the highest one.

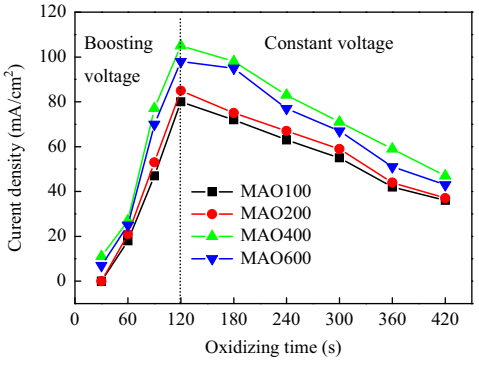

Fig. 4. Changes in the current density during the MAO process for various porous titanium substrates prepared by vacuum sintering titanium beads with different diameters.

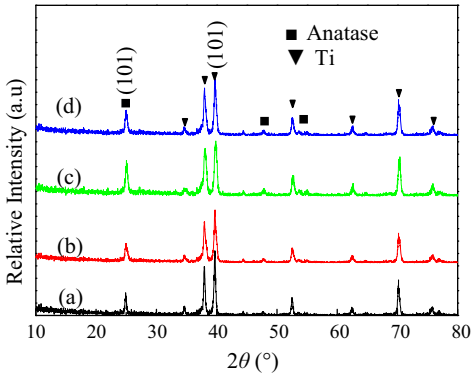

Fig. 5. XRD patterns of the MAO coatings on the porous titanium prepared by vacuum sintering titanium beads with different diameters: (a) MAO100, (b) MAO200, (c) MAO400 and (d) MAO600.

Table 1
The diffraction intensity ratio between the (101) crystal plane of anatase and the (101) crystal plane of titanium.

Samples	Intensity ratio
MAO100	0.34
MAO200	0.35
MAO400	0.60
MAO600	0.42

3.3. Phase composition of the MAO coatings

Fig. 5 shows the XRD patterns of the MAO coatings on the porous titanium prepared by vacuum sintering titanium beads with diameters of 100, 200, 400 and 600 μm. Diffraction peaks of anatase were observed on the all MAO coatings. Table 1 shows the diffraction intensity ratio between the (101) crystal plane of anatase and the (101) crystal plane of titanium. It can be seen that the diffraction intensity ratio increases from 0.34 to 0.60 with the varied titanium beads diameters from 100 to 400 μm. However, when the titanium beads diameter further increased to 600 μm, the diffraction intensity ratio decreased to 0.42. This result implies a fact that the deposition of anatase on the MAO400 sample is relatively easily compared to the other coatings.

3.4. Surface morphology of porous titanium after MAO treatment

Fig. 6 shows the surface morphology (at low magnification) of the MAO coatings on porous titanium composed of different diameter titanium beads. Generally, the MAO technique did not obviously change the shape of the porous titanium. MAO coatings were observed not only at the surface of titanium beads but also in the joints between two titanium beads, although the diameter of titanium beads changed.

Fig. 7 shows the surface morphology of the MAO100 coatings at the joint regions among titanium beads. Obviously, these regions were all oxidized completely. And no significant difference in MAO coating surface can be observed between bead surface and interconnected area.

Fig. 8 shows the surface morphology (at high magnification) of the MAO coatings on porous titanium composed by different diameter titanium beads respectively. The MAO coatings exhibit a porous structure, which is beneficial to cell attachment, propagation and bone growth [29]. The micropores, like volcanic vent, formed during microarc discharge process, are distributed in regular intervals on all MAO coatings. It was interesting that the number of micropores on the MAO coating declined but the sizes of the micropores increased with the varied diameter of titanium beads from 100 to 400 μm (Fig. 9). However, when the diameter of titanium bead reached at 600 μm, the number of micropores on the MAO coating began to increase, while the sizes of micropores decreased. The results indicate that the diameter of titanium bead has a significant effect on the surface morphology of the MAO coatings in the present electrolyte.

3.5. Elemental composition of the MAO coatings

Fig. 10 shows the elemental composition and concentrations of the MAO coatings on porous titanium. The elemental compositions of all the MAO coatings are Ti, O, Si, Ca and Na. It can be seen that the concentrations of Ca and Si of the MAO coating increase but those of Ti and O decrease, when the diameter of titanium beads varies from 100 to 400 μm (Fig. 10). However, with the further increasing of titanium bead diameter to 600 μm, the concentrations of Ca and Si of the MAO coating begin to decrease, while those of Ti and O of the MAO coating increase. Compared to other elements, the change in the Na concentration is not significant.

4. Discussion

In this paper, porous Ti was prepared by vacuum sintering Ti plates covered by titanium beads with different diameters. The formation and structures of MAO coatings on porous Ti have been investigated. According to the current results, it can be found that the effects of titanium beads diameters on the MAO processing current density, porosity, specific surface, phase composition, surface morphology and elemental concentrations are significant. It is very interesting that the titanium beads diameters is how to affect the structures of MAO coatings. Firstly, in the preparation, only the titanium beads diameter of the porous Ti has changed, which directly leads to the changes in two parameters of specific surface area and porosity. Then, the changes of specific surface area and porosity could further affect the structures of MAO coatings.

According to the formation mechanism of MAO coatings, the effect of specific surface area can be described as the reduction for electric breakdown due to enlarge of the surface area based on the same sample volume. Thus, the electric breakdown becomes dispersed, resulting in the decline of growth ability for MAO coatings, and the similar appearance can be observed from the morphology in Fig. 8(a)–(c).

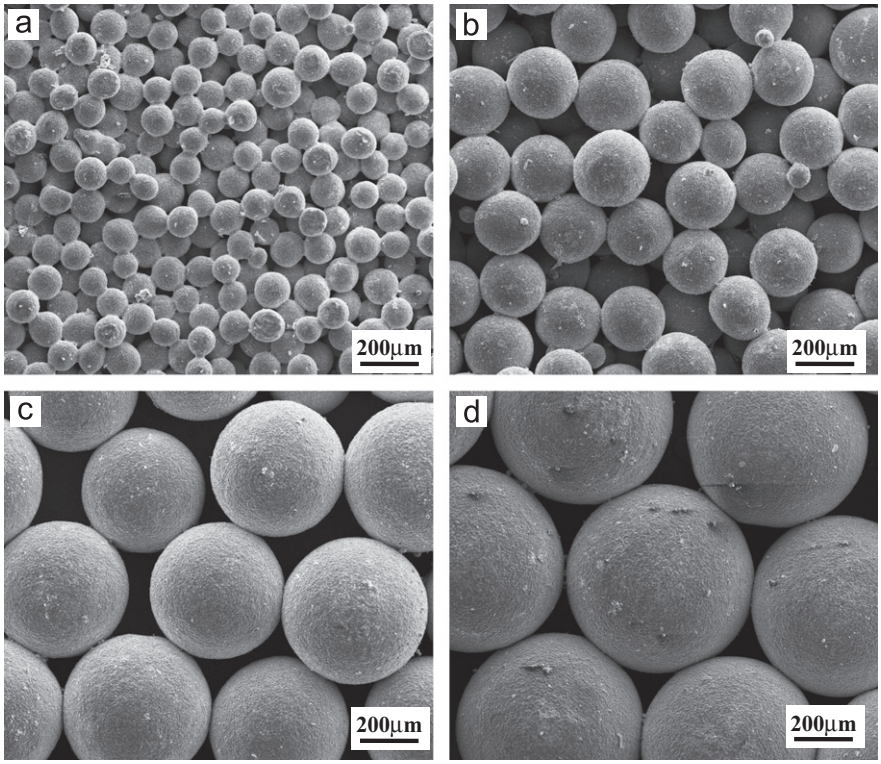

Fig. 6. SEM morphology at low magnification of the MAO coatings on the porous titanium prepared by vacuum sintering titanium beads with different diameters: (a) MAO100, (b) MAO200, (c) MAO400 and (d) MAO600.

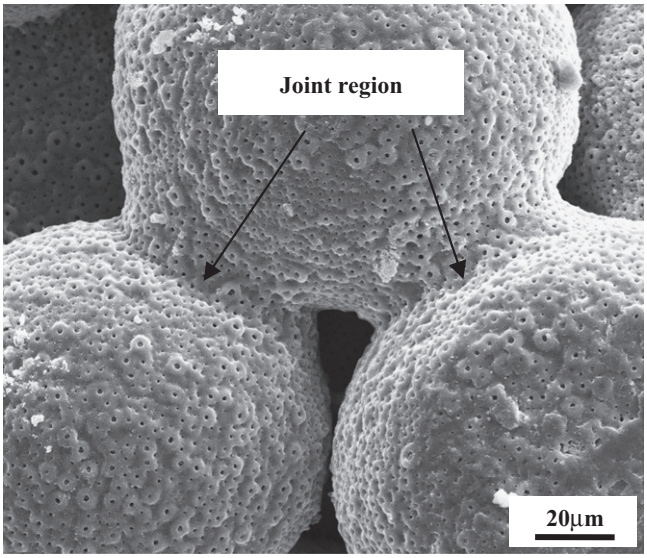

Fig. 7. SEM morphology of the MAO100 coatings at the joint region among titanium beads.

Meanwhile, the increasing of specific surface area also can be considered as the reason for the decrease of ions concentration on unit area. Because the porous Ti prepared by various titanium beads with different diameters has different surface area at the same sample volume, the ions concentrations on unit area are different in the same electrolyte. Thus, in the case of the porous Ti with low specific surface area, the ions concentration on unit area is higher compared to that with high specific surface area. This is the reason why the current density increases with increasing the titanium beads diameters from 100 to 600 μm as shown in Fig. 4, due to the decreasing of specific surface area. Namely, the decline of specific surface area improves the oxidizing ability on porous Ti surfaces.

At the same time, the formation of coatings also may be influenced by the porosity of samples. As liquid, the electrolyte is very easy to flow into the hollow caused by porous Ti, leading to the change of electric resistance. The electrolyte would be considered as reinforcement with much higher resistance, and linked with the Ti in form of series circuits based on the structure analysis (Fig. 11). Fig. 11(a) shows an imaginary sample with same size compared to titanium plate covered titanium beads. However, the layer of titanium beads was replaced by a compact titanium layer in Fig. 11(a). With increasing the titanium beads diameter, the porosity of porous titanium layer increased, the much more electrolyte filled with the porosity, thus it decreased the conduction ability between titanium beads. Namely, the system resistance is composed of R_{Ti} and $R_{Electrolyte}$ as shown in Fig. 11(d), where the R_{Ti} included the titanium plate and beads. Apparently, the resistance of sample structure in Fig. 11(a) is lower than that of sample structure in Fig. 11(b) and Fig. 11(c), since the R_{Ti} is lower than $R_{Electrolyte}$. At the same time, the resistance of sample structure increased with increasing the titanium beads, which resulted in the decline of current at the same applied voltages and further caused the attenuate of oxidizing ability.

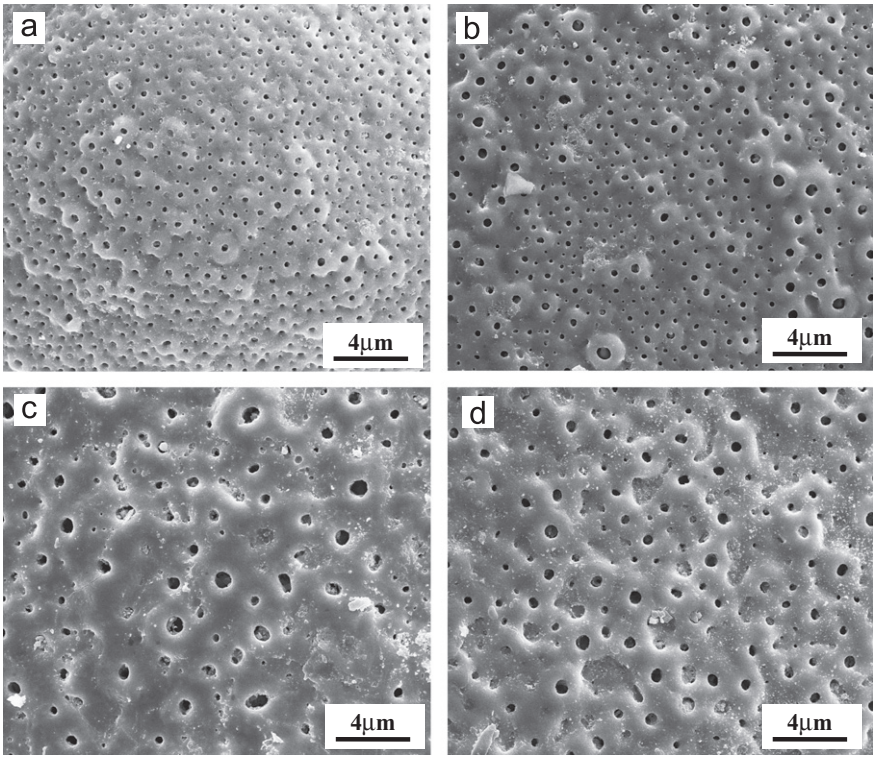

Fig. 8. SEM morphology at high magnification of the MAO coatings on the porous titanium prepared by vacuum sintering titanium beads with different diameters: (a) MAO100, (b) MAO200, (c) MAO400 and (d) MAO600.

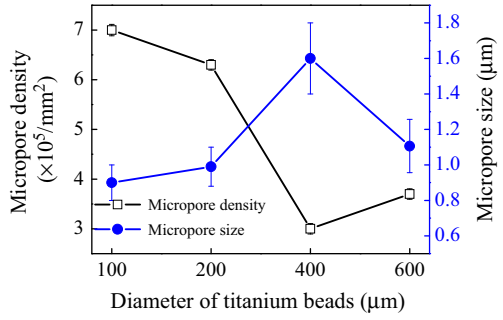

Fig. 9. Micropore density and size of the MAO coatings on porous titanium prepared by vacuum sintering titanium beads with different diameters of 100, 200, 400 and 600 μm.

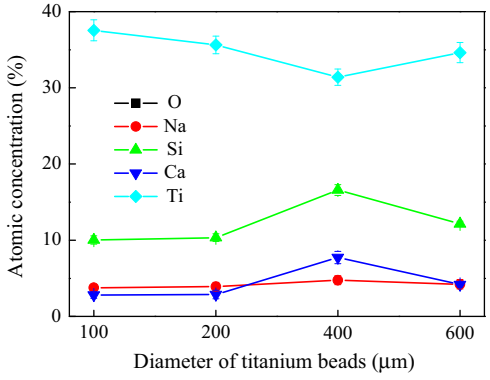

Fig. 10. Elemental composition and concentrations of the MAO coatings on porous titanium prepared by vacuum sintering titanium beads with different diameters of 100, 200, 400 and 600 μm.

Associated considered the two parameters, as the oxidizing ability is positive correlated with bead diameter as porosity but negative correlated with bead diameter as specific surface area, a comprehensive model comes out as shown in Fig. 12. At the relatively low sphere diameter, smaller than 400 μm, because of the dramatic rise in specific surface area but little change in electric resistance related to porosity, the oxidizing ability is dominated by specific surface area, showing a rise trend with sphere diameter as shown by curve b and c in Fig. 12. Hence, when the sphere diameter reach to 400 μm, the leading dominant parameter shifts to porosity as the sharply increased electric resistance caused by the influx electrolyte in certain volume. So, the oxidizing ability would decrease with the rise sphere diameter lager than 400 μm as shown in Fig. 12 of curve c. The curve c is a merging of curve a and b, p, presenting a phenomenon of first increasing and then decreasing in oxidizing ability with rising the diameter of titanium beads. Obviously, when the oxidizing ability increased, the current density, titania concentration, micropore size, Si and Ca elemental concentrations increased. Conversely, these parameters declined when the oxidizing ability decreased. Thus, these parameters reach a maximum when diameter of titanium beads is 400 μm. Generally, the MAO on the surface of porous materials is complex, which has less reported according to current investigation. In this paper, the porosity and specific surface area possibly are two key factors to influence the formation and microstructures of

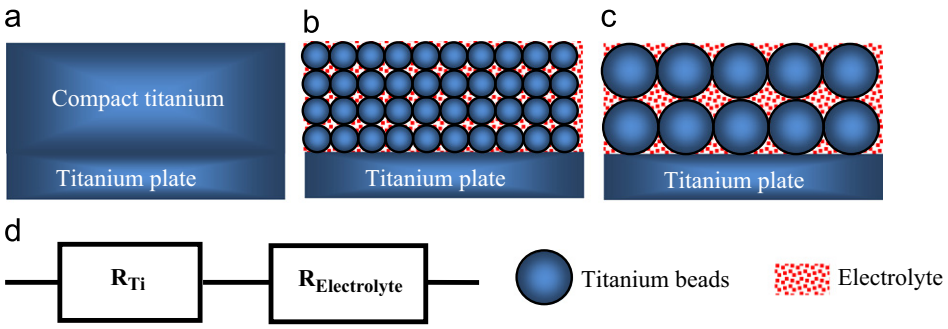

Fig. 11. Schematic diagram for resistor connected form based on structure analysis: (a) an imaginary sample with same size compared to titanium plate covered titanium beads, (b) the structure of the Ti beads with small size of diameter sintered on titanium plate, (c) the structure of the Ti beads with big size of diameter sintered on titanium plate and (d) series circuits for resistors of Ti and electrolyte.

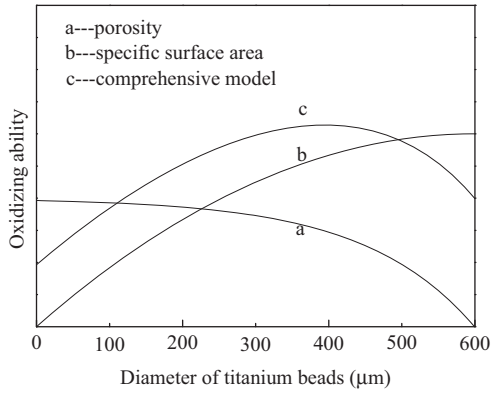

Fig. 12. Schematic diagram for effect of porosity and specific surface area of porous titanium formed by titanium beads with different diameters on oxidizing ability.

MAO coatings. Further investigations on these issues have been done, which could be report later.

5. Conclusion

TiO_2-based coatings containing Si, Ca, Na (SCN) elements were formed on porous titanium by micro-arc oxidation (MAO). The titanium beads diameter directly determined two parameters of porosity and specific surface area of porous titanium. The surface morphology, SCN concentrations and titania concentration of the MAO coatings were significantly affected by the diameter of titanium beads due to the change in porosity and specific surface area of porous titanium. Associated considered the two parameters, as the oxidizing ability is positive correlated with bead diameter as porosity but negative correlated with bead diameter as specific surface area. When the oxidizing ability increased, the current density, titania concentration, micropore size, SCN concentrations increased. Conversely, these parameters declined when the oxidizing ability decreased.

Acknowledgments

This work was financially supported by National Natural Science Foundation of China (Grant nos. 51002039 and 51021002), Fund for the Doctoral Project to New Teachers and National Basic Science Research Program (2012CB933900).

References

[1] M.C. Melican, M.C. Zimmerman, M.S. Dhillon, A.R. Ponnambalam, A. Curodeau, J.R. Parsons, Three-dimensional printing and porous metallic surfaces: a new orthopedic application, Journal of Biomedical Materials Research 55 (2) (2001) 194–202.

[2] J.P. Li, P. Habibovic, M. van den Doel, C.E. Wilson, J.R. de Wijn, C.A. van Blitterswijk, K. de Groot, Bone ingrowth in porous titanium implants produced by 3D fiber deposition, Biomaterials 28 (18) (2007) 2810–2820.

[3] G. Ryan, A. Pandit, D.P. Apatsidis, Fabrication methods of porous metals for use in orthopaedic applications, Biomaterials 27 (13) (2006) 2651–2670.

[4] X.Y. Liu, P.K. Chu, C.X. Ding, Surface modification of titanium, titanium alloys, and related materials for biomedical applications, Materials Science and Engineering R: Reports 47 (3–4) (2004) 49–121.

[5] D.A. Puleo, R.A. Kissling, M.S. Sheu, A technique to immobilize bioactive proteins, including bone morphogenetic protein-4 (BMP-4), on titanium alloy, Biomaterials 23 (9) (2002) 2079–2087.

[6] K. Das, S. Bose, Surface modifications and cell-materials interactions with anodized Ti, Acta Biomaterialia 3 (4) (2007) 573–585.

[7] A.L. Yerokhin, X. Nie, A. Leyland, A. Matthews, S.J. Dowey, Plasma electrolysis for surface engineering, Surface and Coatings Technology 122 (2–3) (1999) 73–93.

[8] A. Ghasemi, V.S. Raja, C. Blawert, W. Dietzel, K.U. Kainer, The role of anions in the formation and corrosion resistance of the plasma electrolytic oxidation coatings, Surface and Coatings Technology 204 (9-10) (2010) 1469–1478.

[9] A. Ghasemi, V.S. Raja, C. Blawert, W. Dietzel, K.U. Kainer, Study of the structure and corrosion behavior of PEO coatings on AM50 maginesium. alloy by electrochemical impedance spectroscopy, Surface and Coatings Technology 202 (15) (2008) 3513–3518.

[10] Y.L. Cheng, F. Wu, E. Matykina, P. Skeldon, G.E. Thompson, The influences of microdischarge types and silicate on the morphologies and phase compositions of plasma electrolytic oxidation coatings on Zircaloy-2, Corrosion Science 59 (2012) 307–315.

[11] Y.M. Wang, D.C. Jia, L.X. Guo, T.Q. Lei, B.L. Jiang, Effect of discharge pulsating on microarc oxidation coatings formed on Ti6Al4V alloy, Materials Chemistry and Physics 90 (1) (2005) 128–133.

[12] Y.M. Wang, B.L. Jiang, T.Q. Lei, L.X. Guo, Microarc oxidation coatings formed on Ti6A14V in Na_2SiO_3 system solution: microstructure, mechanical and tribological properties, Surface and Coatings Technology 201 (1–2) (2006) 82–89.

[13] D.Q. Wei, Y. Zhou, D.C. Jia, Y.M. Wang, Characteristic and in vitro bioactivity of a microarc-oxidized TiO2-based coating after chemical treatment, Acta Biomaterialia 3 (5) (2007) 817–827.
[14] D.Q. Wei, Y. Zhou, D.C. Jia, Y.M. Wang, Effect of heat treatment on the structure and in vitro bioactivity of microarc-oxidized (MAO) titania coatings containing Ca and P ions, Surface and Coatings Technology 201 (21) (2007) 8723–8729.
[15] D.Q. Wei, Y. Zhou, D.C. Jia, Y.M. Wang, Effect of applied voltage on the structure of microarc oxidized TiO_2-based bioceramic films, Materials Chemistry and Physics 104 (1) (2007) 177–182.
[16] M. Fini, A. Cigada, G. Rondelli, R. Chiesa, R. Giardino, G. Giavaresi, N.N. Aldini, P. Torricelli, B. Vicentini, In vitro and in vivo behaviour of Ca- and P-enriched anodized titanium, Biomaterials 20 (17) (1999) 1587–1594.
[17] X.L. Zhu, K.H. Kim, Y.S. Jeong, Anodic oxide films containing Ca and P of titanium biomaterial, Biomaterials 22 (16) (2001) 2199–2206.
[18] X.L. Zhu, J.L. Ong, S. Kim, K. Kim, Surface characteristics and structure of anodic oxide films containing Ca and P on a titanium implant material, Journal of Biomedical Materials Research 60 (2) (2002) 333–338.
[19] I.H. Oh, N. Nomura, N. Masahashi, S. Hanada, Mechanical properties of porous titanium compacts prepared by powder sintering, Scripta Materialia 49 (12) (2003) 1197–1202.
[20] G.A. Murray, J.C. Semple, Transfer of tensile loads from a prosthesis to bone using porous titanium, Journal of Bone and Joint Surgery 63-B (1981) 138–141.
[21] M. Bram, C. Stiller, H.P. Buchkremer, D. Stover, H. Baur, High-porosity titanium, stainless steel, and superalloy parts, Advanced Engineering Materials 2 (4) (2000) 196–199.
[22] C.E. Wen, M. Mabuchi, Y. Yamada, K. Shimojima, Y. Chino, T. Asahina, Processing of biocompatible porous Ti and Mg, Scripta Materialia 45 (10) (2001) 1147–1153.
[23] B. Gorny, T. Niendorf, J. Lackmann, M. Thoene, T. Troester, H.J. Maier, In situ characterization of the deformation and failure behavior of non-stochastic porous structures processed by selective laser melting, Materials Science and Engineering A 528 (2011) 7962–7967.
[24] L. Markus, H. Simon, M. Wilhelm, W. Konrad, S. Ralf, T. Rainer, P. Reinhart, F. Horst, Manufacturing of individual biodegradable bone substitute implants using selective laser melting technique, Journal of Biomedical Materials Research Part A 97A (2011) 466–471.
[25] H. Nikolas, H. Peter, F. Brian, K. Carolin, B. Rajendra, Compression–compression fatigue of selective electron beam melted cellular titanium (Ti–6Al–4V), Journal of Biomedical Materials Research Part B 99B (2011) 313–320.
[26] S. Cheng, D.Q. Wei, Y. Zhou, H.F. Guo, Preparation, cell response and apatite-forming ability of microarc oxidized coatings containing Si, Ca and Na on titanium, Ceramics International 37 (7) (2011) 2505–2512.
[27] S. Cheng, D.Q. Wei, Y. Zhou, Structure of microarc oxidized coatings containing Si, Ca and Na on titanium and deposition of cefazolin sodium/chitosan composite film, Surface and Coatings Technology 205 (13–14) (2011) 3798–3904.
[28] S. Cheng, D.Q. Wei, Y. Zhou, H.F. Guo, Characterization and properties of microarc oxidized coatings containing Si, Ca and Na on titanium, Ceramics International 37 (6) (2011) 1761–1768.
[29] L.H. Li, Y.M. Kong, W.H. Kim, Y.W. Kim, Improved biological performance of Ti implants due to surface modification by micro-arc oxidation, Biomaterials 25 (14) (2004) 2867–2875.